HHS Public Access

Author manuscript

J Periodontal Res. Author manuscript; available in PMC 2023 January 01.

Published in final edited form as:

J Periodontal Res. 2022 January ; 57(1): 173–185. doi:10.1111/jre.12951.

Inhibition of Acid Sphingomyelinase by Imipramine Abolishes the Synergy between Metabolic Syndrome and Periodontitis on Alveolar Bone Loss

Yanchun Li[1], **Zhongyang Lu**[1], **Lixia Zhang**[2], **Cameron L. Kirkwood**[2], **Keith L. Kirkwood**[2,3], **Maria F. Lopes-Virella**[1,4], **Yan Huang**[1,4,*]

[1]Division of Endocrinology, Diabetes and Medical Genetics, Department of Medicine, College of Medicine, Medical University of South Carolina, Charleston, SC 29425

[2]Department of Oral Biology, School of Dental Medicine, University at Buffalo,

[3]Department of Head and Neck/Plastic and Reconstructive Surgery, Roswell Park Comprehensive Cancer Center, Buffalo, NY 14214

[4]Ralph H. Johnson Veterans Affairs Medical Center, Charleston, SC 29401

Abstract

Background and objective: Clinical studies have shown that metabolic syndrome (MetS) exacerbates periodontitis. However, the underlying mechanisms remain largely unknown. Since our animal study has shown that high-fat diet-induced MetS exacerbates lipopolysaccharide (LPS)-stimulated periodontitis in mouse model and our *in vitro* study showed that acid sphingomyelinase (aSMase) plays a key role in the amplification of LPS-triggered pro-inflammatory response by palmitic acid (PA) in macrophages, we tested our hypothesis that inhibitor of aSMase attenuates MetS-exacerbated periodontitis in animal model. Furthermore, to explore the potential underlying mechanisms, we tested our hypothesis that aSMase inhibitor downregulates pro-inflammatory and pro-osteoclastogenic gene expression in macrophages *in vitro*.

Material and methods: We induced MetS and periodontitis in C57BL/6 mice by feeding high-fat diet (HFD) and periodontal injection of A. *actinomycetemcomitans* LPS, respectively, and treated mice with imipramine, a well-established inhibitor of aSMase. Micro-computed tomography (microCT), tartrate-resistant acid phosphatase staining, histological and pathological evaluations as well as cell cultures were performed to evaluate alveolar bone loss, osteoclast formation, periodontal inflammation and pro-inflammatory gene expression.

[*]Correspondence to Yan Huang, M.D., Ph.D., Ralph H. Johnson Veterans Affairs Medical Center, and Division of Endocrinology, Diabetes and Medical Genetics, Department of Medicine, Medical University of South Carolina, 114 Doughty St. Charleston, SC29403, Tel: (843) 789-6824; Fax: (843) 876-5133; huangyan@musc.edu.

AUTHORS' CONTRIBUTION

The study was designed by YH. Laboratory work was done by YL and ZL. Tissue analysis was directed and performed by KLK, LZ and MLK. The manuscript was drafted by YH and finalized by KLK, MFL and YH. The manuscript was reviewed and approved by YL, ZL, LZ, KLK, MLK, MFL and YH.

CONFLICT INTEREST

The authors declare that they have no conflicts of interest.

Results: Analysis of metabolic parameter showed that while HFD induced MetS by increasing bodyweight, insulin resistance, cholesterol and free fatty acids, imipramine reduced free fatty acids but had no significant effects on other metabolic parameters. MicroCT showed that either MetS or periodontitis significantly reduced bone volume fraction (BVF) of maxilla and the combination of MetS and periodontitis further reduced BVF. However, imipramine increased BVF in mice with both MetS and periodontitis to a level similar to that in mice with periodontitis alone, suggesting that imipramine abolished the synergy between MetS and periodontitis on alveolar bone loss. Consistently, results showed that imipramine inhibited osteoclast formation and periodontal inflammation in mice with both MetS and periodontitis. To elucidate the mechanisms by which imipramine attenuates MetS-exacerbated periodontitis, we showed that imipramine inhibited the upregulation of pro-inflammatory cytokines and transcription factor c-FOS as well as ceramide production by LPS plus PA in macrophages.

Conclusion: This study has shown that imipramine as an inhibitor of aSMase abolishes the synergy between MetS and periodontitis on alveolar bone loss in animal model and inhibits pro-inflammatory and pro-osteoclastogenic gene expression in macrophages *in vitro*. This study provides the first evidence that aSMase is a potential therapeutic target for MetS-exacerbated periodontitis.

Keywords

Metabolic Syndrome; Periodontitis; Imipramine; Acid Sphingomyelinase; Inflammation

1. INTRODUCTION

Periodontitis is a primarily bacterial infection of the supporting structures of teeth, characterized by periodontal inflammation and alveolar bone loss that eventually lead to tooth loss (1, 2). Metabolic syndrome (MetS) is a cluster of cardiovascular risk factors including abdominal obesity, atherogenic dyslipidemia, hypertension, insulin resistance, pro-inflammatory and prothrombotic state (3), and highly predictive of new-onset type 2 diabetes (3, 4). While type 2 diabetes is well known as an independent risk factor for periodontitis (5), MetS has been also shown to be associated with periodontitis (6). Although it has been reported that the association between MetS and periodontitis is the result of MetS-increased systemic oxidative stress and inflammatory response (7), the underlying mechanisms and potential targets to interrupt MetS-periodontitis crosstalk remain largely unknown.

In our study to understand the mechanisms involved in MetS-exacerbated periodontitis, we have focused on macrophages since macrophages play a central role in periodontal inflammation, osteoclastogenesis, alveolar bone loss and restoration of tissue homeostasis (8–10). We found that sphingolipid metabolism, in particular sphingomyelin (SM) hydrolysis pathway, is involved in the crosstalk between lipopolysaccharide (LPS) and saturated fatty acids (SFAs) such as palmitic acid (PA) in macrophages (11). We observed that SFAs, which contribute to the pathogenesis of MetS (12), cooperate with LPS to stimulate acid sphingomyelinase (aSMase) and subsequent ceramide (CER) production, leading to the augmentation of LPS-induced inflammatory signaling (11). We also observed that targeting aSMase *in vitro* with imipramine, a commonly-used pharmacological inhibitor

of aSMase (13–15), strongly inhibited the synergistic effect of LPS and SFA on macrophage inflammatory signaling (11).

In the current study, we used a mouse model with MetS-exacerbated periodontitis, which we established previously (16), to test our hypothesis that imipramine attenuates MetS-exacerbated periodontitis in animal model. We also tested our hypothesis that imipramine downregulates pro-inflammatory and pro-osteoclastogenic gene expression in macrophages *in vitro*.

2. MATERIALS AND METHODS

2.1 Animal feeding and treatment

Six weeks old male C57BL/6 mice were purchased from Taconic Farms (Hudson, New York, USA) and randomly divided into 8 groups: (1) Control; (2) Control with aSMase inhibition; (3) Periodontitis; (4) Periodontitis with aSMase inhibition; (5) MetS; (6) MetS with aSMase inhibition; (7) Periodontitis and MetS; (8) Periodontitis and MetS with aSMasae inhibition. Each group had 7–10 mice. MetS was induced in mice by feeding high-fat diet (HFD) (D12492, 60 kcal% fat) (Research Diets, Inc., New Brunswick, NJ) for 20 weeks. Control mice were fed low-fat diet (LFD) (D12450J, 10 kcal% fat). Both D12450J and D12492 diets contain 7% sucrose. The mice were housed with a 12-hour light/12-hour dark cycle and had free access to tap water and food. During the last 4 weeks of LFD or HFD feeding, periodontitis was induced in mice by injecting LPS isolated from A. *actinomycetemcomitans* (strain Y4, serotype B) (17) (10 μg of LPS per mouse) through both left and right sides of the palatal gingiva between the maxillary 1st and 2nd molars, 3 times per week as described previously (18, 19). For control, mice were periodontally injected with phosphate-buffered saline (PBS), the vehicle for LPS. To inhibit aSMase, imipramine (Sigma, St. Louis, MO) at 10 μg/g bodyweight was given to half mice by daily intraperitoneal injection 3 weeks before and 4 weeks during the LPS injection and PBS was injected for control mice. The Institutional Animal Care and Use Committee at the Medical University of South Carolina approved all experimental protocols. All animal-related work was performed in accordance with ARRIVE guidelines for preclinical studies and the National Institute of Health Guidelines.

2.2 Metabolic measurements

Blood samples were obtained under the fasted condition and glucose level was determined using a Precision QID glucometer (MediSense Inc., Bedford, MA). Serum cholesterol and triglycerides were measured using Cholestech LDX Lipid monitoring System (Fisher Scientific, Pittsburgh PA). Serum free fatty acids (FFAs) were determined using the EnzyChrom™ free fatty acid kit (BioAssay systems, Hayward, CA). Serum fasting insulin was assayed using the Ultra Sensitive Insulin ELISA Kit (Crystal Chem, Inc., Downers Grove, IL). Fasting whole body insulin sensitivity was estimated with the homeostasis model assessment of insulin resistance (HOMA-IR) according to the formula [fasting plasma glucose (mg/dL) × fasting plasma insulin (μU/mL)]/405.

2.3 Micro-computed tomography (μCT) and bone volume fraction (BVF) analysis

Maxillae were fixed in 10% phosphate-buffered formalin for 24h, washed with PBS, and stored in 70% ethanol. Maxillae were scanned at 55kVp, 145uA, 16um voxel resolution using Scanco Medical 40 uCT scanner (Scanco Medical, Brüttisellen, Switzerland) in the MUSC Center for Oral Health as described previously (20). 3-dimensional images were generated and reconstructed for each specimen. These images were rotated with a standard orientation and threshold to discern mineralized and non-mineralized tissue. The region of interest (ROI) was indicated by the contour height of molars at the cementoenamel junction as the width and the molar cusp tips to root apices as the height. Depth was equal to the buccolingual size of the teeth plus 1.0 mm^3. Bone volume fraction was calculated as the percentage of bone within the ROI using AnalyzePro software (Seattle, WA). Data are reported in accordance with standardized nomenclature (21). Additionally, three liner measurements of the distance from the cemento-enamel junction (CEJ) to the alveolar bone crest (ABC) were taken for the first and second molars as described previously (22).

2.4 Tartrate-resistant acid phosphatase (TRAP) staining and quantification of osteoclasts

Formalin-fixed maxillae were decalcified in a 10% EDTA solution for 4 weeks at 4°C. The EDTA solution was changed three times per week. The maxillae were paraffin-embedded and 7 μm sagittal sections were prepared. TRAP staining was performed in tissue sections using a leukocyte acid phosphatase kit (Sigma Aldrich, St. Louis, MO, USA). The tissue sections were counterstained with hematoxylin after TRAP staining. Active osteoclasts were defined as multinucleated TRAP-positive cells in contact with bone surface. TRAP-positive osteoclasts under the first and the second molar on the surface of alveolar bone in five random sections from each mouse were counted. A well-trained and experienced research specialist who was blinded to the treatment groups counted the TRAP-positive cells.

2.5 Histological tissue processing and pathological evaluation

The above paraffin-embedded sections in a bucco-palatal orientation were stained with hematoxylin and eosin to evaluate periodontal architecture and inflammatory status in the area between the first and second molars. A calibred, well-trained and experienced research specialist who was blinded to the treatment groups evaluated the tissue inflammation and bone resorption according to the criteria for scoring tissue inflammation and bone resorption: 0 = within normal limits; 1 = focal some leukocyte infiltration, no significant bone resorption; 2 = moderate leukocyte infiltration with mild bone resorption; 3 = severe leukocyte infiltration with moderate bone resorption; and 4 = severe leukocyte infiltration with extensive bone resorption (23).

2.6 Cell culture

RAW264.7 macrophages were purchased from the American Type Culture Collection (ATCC, Manassas, VA) and grown in DMEM (ATCC, Manassas, VA) supplemented with 10% heat-inactivated fetal calf serum (HyClone, Logan, UT). The cells were maintained in a 37 °C, 90% relative humidity, 5% CO_2 environment. A. *actinomycetemcomitans* LPS, PA and imipramine were used for cell treatment.

2.7 PA preparation

To prepare PA for cell treatments, PA (Sigma, St. Louis, MO) was dissolved in 0.1 N NaOH and 70% ethanol at 70°C to make PA with stock concentration of 50 mM. The solution was kept at 55°C for 10 min, mixed and brought to room temperature.

2.8 Enzyme-linked immunosorbent assay (ELISA)

Interleukin (IL)-6 in medium was quantified using a sandwich ELISA kit according to the protocol provided by the manufacturer (Biolegend, San Diego, CA).

2.9 PCR array

The expression of the biomarkers for periodontitis including colony-stimulating factor 2 (CSF2), C-X-C motif chemokine 10 (CXCL10), interleukin 1 alpha (IL-1α) and interleukin 1 beta (IL-1β) and tumor necrosis factor (TNF) were quantified using PCR array. First-strand cDNA was synthesized from RNA using RT2 First Strand Kit (SuperArray Bioscience Corp., Frederick, MD). Mouse Toll-like receptor (TLR) pathway-focused PCR Arrays (SuperArray Bioscience Corp.) were performed using 2X SuperArray RT^2 qPCR master mix and the first strand cDNA by following the instructions from the manufacturer.

2.10 RNA isolation and quantitative real-time polymerase chain reaction (PCR)

Total RNA was isolated from cells using the RNeasy minikit (Qiagen, Santa Clarita, CA). First-strand complementary DNA (cDNA) was synthesized with the iScript cDNA synthesis kit (Bio-Rad Laboratories, Hercules, CA) using 20 μl of the reaction mixture containing 0.5 μg of total RNA, 4 μl of 5x iScript reaction mixture, and 1 μl of iScript reverse transcriptase. The complete reaction was cycled for 5 min at 25°C, 30 min at 42°C, and 5 min at 85°C using a PTC-200 DNA Engine (MJ Research, Waltham, MA). The reverse transcription reaction mixture was then diluted 1:10 with nuclease-free water and used for PCR amplification in the presence of the primers. Real-time PCR was performed as described previously (11). The Beacon designer software (PREMIER Biosoft International, Palo Alto, CA) was used for primer designing (mouse c-FOS: 5’ primer sequence, CGGGTTTCAACGCCGACTA; 3’ primer sequence, TGGCACTAGAGACGGACAGAT. Primers were synthesized by Integrated DNA Technologies, Inc. (Coralville, IA). Mouse glyceraldehyde 3-phosphate dehydrogenase (GAPDH) was used as a control (5’ primer sequence, CTGAGTACGTCGTGGAGTC; 3’ primer sequence, AAATGAGCCCCAGCCTTC). Data were analyzed with the iCycler iQ™ software. The average starting quantity (SQ) of fluorescence units was used for analysis. Quantification was calculated using the SQ of ASMase cDNA relative to that of GAPDH cDNA in the same sample.

2.11 Lipidomics

RAW264.7 cells were collected, fortified with internal standards, extracted with ethyl acetate/isopropyl alcohol/water (60:30:10, v/v/v), evaporated to dryness, and reconstituted in 100 μl of methanol. Simultaneous ESI/MS/MS analyses of sphingoid bases, sphingoid base 1-phosphates, CERs, and SMs were performed on a Thermo Finnigan TSQ 7000 triple quadrupole mass spectrometer operating in a multiple reaction monitoring positive

ionization mode. The phosphate contents of the lipid extracts were used to normalize the MS measurements of sphingolipids. The phosphate contents of the lipid extracts were measured with a standard curve analysis and a colorimetric assay of ashed phosphate (24).

2.12 Statistic analysis

GraphPad Prism 8 (Version 8.4.3) (GraphPad Software, Inc. La Jolla, CA) was used for statistical analysis. The one-way analysis of variance (ANOVA) with the post hoc test was used to determine whether there are any statistically significant differences between the means of three or more independent groups. Student t test was performed for comparison between two groups when the data had normal distribution. For data without normal distribution, nonparametric analysis using Mann-Whitney test was performed. When an experiment was repeated, statistical analysis was also performed to compare their variances. The values were expressed as mean ± SD and a value of $P < 0.05$ was considered significant.

3. RESULTS

3.1 The effect of imipramine on metabolic parameters

Results from the tests on metabolic parameters showed that HFD feeding for 20 weeks induced MetS as mice had increases in bodyweight, insulin, insulin resistance (HOMA-IR) and lipids including cholesterol and free fatty acids (Fig. 1), which are similar to the findings from our previous report (16). Additionally, periodontitis induced by periodontal LPS injection during the last 4 weeks did not significantly alter the effect of MetS on the parameters (Fig. 1). Furthermore, imipramine had no significant effect on the serum metabolic parameters except free fatty acids (Fig 1), suggesting that imipramine treatment did not improve MetS.

3.2 Imipramine attenuates MetS-exacerbated alveolar bone loss

We performed microCT scanning on maxillae to show alveolar bone with teeth (Fig. 2A) and quantify BVF (Fig. 2B). To show the effect of imipramine on alveolar bone loss in mice with MetS and/or periodontitis, we determined both BVF (Fig. B) and CEJ-ABC distances (Fig. 2C). We also demonstrated the CER-ABC distance of the first and second molars (Fig. 2D). Results showed that, without imipramine treatment, either periodontitis or MetS significantly decreased BVF and increased CEJ-ABC distance, and the combination of periodontitis and MetS further decreased BVF and increased CEJ-ABC distance (Fig. 2A, B and C). These results are consistent with those reported by our previous study (16) and underscore the exacerbation of periodontitis by MetS. Furthermore, imipramine treatment significantly decreased BVF and increased CEJ-ABC distance in the control mice but had no significant effect on BVF in mice with periodontitis or MetS alone (Fig. 2A, B and C). Interestingly, imipramine markedly increased BVF and decreased CEJ-ABC distance in mice with both periodontitis and MetS to the levels similar to those in mice with periodontitis alone (Fig. 2A, B and C), suggesting that imipramine treatment abolished the synergy between MetS and periodontitis on alveolar bone loss.

3.3 Imipramine attenuates osteoclastogenesis induced by both periodontitis and MetS

To understand how imipramine attenuated alveolar bone loss in mice with both periodontitis and MetS, we performed TRAP staining on tissue sections of maxillae to detect osteoclasts. Results showed that, without imipramine treatment, periodontitis or MetS increased TRAP positive cells and the combination of periodontitis and MetS further increased TRAP positive cells (Fig. 3). Imipramine significantly increased TRAP positive cells in control mice but had no significant effect on TRAP positive cells in mice with periodontitis or MetS (Fig. 3). Remarkably, imipramine decreased TRAP positive cells by 60% in mice with both periodontitis and MetS.

3.4 Imipramine attenuates periodontal inflammation and bone resorption stimulated by both periodontitis and MetS

Histological analysis of maxillae was conducted to determine the inflammatory scores based on leukocyte infiltration and bone resorption in periodontal tissues. We focused on the areas of both periodontal ligaments and subepithelial gingiva (Fig. 4A and B). Results showed that, without imipramine treatment, mice with periodontitis or MetS had increased leukocyte infiltration and bone resorption, and the combination of periodontitis and MetS further increased leukocyte infiltration and bone resorption (Fig. 4C). Furthermore, while imipramine increased leukocyte infiltration and bone resorption in control mice and had no effect in mice with periodontitis or MetS, it significantly attenuated leukocyte infiltration and bone resorption, and thereby reduced inflammatory score in mice with both periodontitis and MetS (Fig. 4C).

3.5 Imipramine inhibits the upregulation of pro-inflammatory cytokines and pro-osteoclastogenic transcription factor in macrophages *in vitro*

To understand the mechanisms by which imipramine abolishes the synergy of MetS and LPS on alveolar bone loss and periodontal inflammation, we performed *in vitro* study to investigate the effect of imipramine on the expression of IL-6 in macrophages stimulated by LPS, PA or both. IL-6 is a major pro-inflammatory cytokine involved in diabetes-related periodontitis (25) and PA is the most abundant SFA in the circulation and increased in patients with obesity or MetS (26). Results showed that while LPS robustly induced IL-6 secretion, PA further boosted LPS-induced IL-6 secretion by RAW264.7 macrophages (Fig. 5A). Results further showed that, in cells treated with both LPS and PA, imipramine reduced IL-6 secretion to the level similar to that in cells stimulated by LPS alone, indicating that imipramine abolished the synergy between PA and LPS on IL-6 expression (Fig. 5A).
We also determined the effect of imipramine on the expression of c-FOS, a transcription factor known to be involved in osteoclast differentiation and osteoclastogenesis (27, 28), in macrophages stimulated by LPS, PA or both. Results showed that while either LPS or PA stimulated c-FOS transcription, the combination of LPS and PA further increased c-FOS mRNA in RAW264.7 macrophages (Fig. 5B). Interestingly, although imipramine increased c-FOS mRNA in control cells, it inhibited the upregulation of c-FOS mRNA stimulated by LPS plus PA by 50% (Fig. 5B). Furthermore, we performed PCR array to determine the effect of imipramine on the expression of a number of pro-inflammatory molecules. Results showed that while LPS and PA synergistically stimulated expression of FOS, IL-1α, IL-1β,

COX-2 and TNFα, imipramine significantly reduced the stimulatory effect of LPS and PA on these molecules (Table 1).

3.6 Imipramine inhibits production of CERs in macrophages in vitro

Since aSMase catalyzes SM hydrolysis that reduces SM content and increases CER production, inhibition of aSMase by imipramine is expected to reduce SM hydrolysis, leading to increased SM content and reduced CER production (Fig. 6A). Indeed, our lipidomic analysis confirmed that while LPS and PA synergistically decreased SM content in macrophages, imipramine significantly increased it (Fig. 6B and Table 2). Furthermore, while LPS and PA synergistically increased CER, imipramine strongly attenuated the effect of LPS and PA on CER production by 46% (Fig. 6C and Table 3).

4. DISCUSSION

We have reported previously that MetS induced by HFD exacerbates LPS-induced periodontitis in C57BL/6 mice (16). The present study used this animal model to show that imipramine, a pharmacological inhibitor of aSMase (29), abolished the synergy between MetS and periodontitis on alveolar bone loss and periodontal inflammation. This finding is important since it demonstrated for the first time that aSMase is a potential target for the treatment of MetS-exacerbated periodontitis. In addition to periodontitis, we have shown recently that amitriptyline, also a pharmacological inhibitor of aSMase, attenuated nonalcoholic steatohepatitis (NASH) and atherosclerosis in a mouse model (30). Given that periodontitis, NASH and atherosclerosis are all complications of MetS (31, 32), these findings suggest that aSMase-related sphingolipid metabolism may be a potential common target for the complications of MetS.

The present study showed that imipramine has no significant effect on HFD-increased bodyweight, insulin, insulin resistance and cholesterol, suggesting that imipramine treatment did not improve MetS. Interestingly, despite lack of improvement on MetS in mice in response to imipramine treatment, the alveolar bone loss and periodontal inflammation were improved significantly. This study thereby indicates that while treatment of MetS by improving bodyweight, insulin resistance and hyperlipidemia certainly improves periodontitis, targeting aSMase to reduce CER and abolish the synergy between MetS and periodontitis on alveolar bone loss and periodontal inflammation is another potential approach to attenuate MetS-exacerbated periodontitis.

To explore the mechanisms involved in the significant reduction of alveolar bone loss and periodontal inflammation by imipramine, our *in vitro* study demonstrated that imipramine effectively inhibited CER production stimulated by the combination of PA and LPS in macrophages. Since it is known that CER, a bioactive sphingolipid, promotes tissue inflammation by activating pro-inflammatory signaling cascades such as nuclear kappa B and mitogen-activated protein kinase pathways (33, 34), these findings indicate that imipramine improves alveolar bone loss and periodontal inflammation by inhibiting CER production and subsequent CER-mediated inflammatory signaling. Therefore, these findings also explain why imipramine is capable of improving MetS-aggravated periodontitis without affecting metabolic disorders.

An intriguing finding from this study is that although imipramine improved periodontitis in mice with both MetS and periodontitis, it worsened alveolar bone loss in the control mice. Actually, this finding is in line with our recent report that aSMase-deficiency in LFD-fed mice exacerbates periodontitis (35). In that study, we found surprisingly that periodontal CER content in mice with aSMase-deficiency was actually increased, but not reduced as expected. Further investigation revealed that the CER increase was due to the activation of CER de novo synthesis via a compensatory mechanism when the baseline level of CER is reduced by lack of SM hydrolysis as a result of aSMase-deficiency (35). Consistently, results from the present study showed that although imipramine increased the content of C16-, C18-, C20-, and C22-SM in the control macrophages as anticipated (Table 1), it did not reduce contents of C16-, C18-, C20-, and C22-CER. In fact, it increased contents of C16-, C18-, C20-, and C22-CER (Table 2), suggesting that CER de novo synthesis was activated in these cells.

It has been reported that increased blood levels of CERs are positively associated with bone resorption markers such as TRAP-5b, bone-specific alkaline phosphatase, nuclear factor kB ligand, and osteoprotegerin (36). Furthermore, *in vitro* study showed that CER directly increased osteoclastogenesis, bone resorption and expression levels of osteoclast differentiation markers (36). Consistently, we showed in the present study that treatment with imipramine in the control macrophages increased both CER level and the expression of c-FOS, a pro-osteoclastogenic transcription factor (Fig. 5B).

Imipramine is an antidepressant for patients with depression (14, 15). Actually, a number of antidepressants including imipramine and amitriptyline are functional inhibitors of aSMase (FIASMAs) (29). Among these drugs, imipramine and amitriptyline belong to the tricyclic antidepressant (TCA) class while other FIASMAs belong to the class of selective serotonin reuptake inhibitor (SSRI) or serotonin-norepinephrine reuptake inhibitor (SNRI). A recent clinical study reported that both SSRI and SNRI had no significant effect on periodontitis (37). Interestingly, Hasan et al. reported recently that periodontal application of 1% amitriptyline gel or 1% amitriptyline mouthwash for 4 weeks reduced periodontal parameters and inflammatory biomarkers in patients with periodontitis (38). Our present study also showed that imipramine attenuated MetS-exacerbated periodontitis in animal model. However, it remains unknown why only TCA antidepressants, but not other classes of antidepressants, have therapeutic effect on periodontitis. It is also unknown if TCA antidepressants improve periodontitis in patients with both MetS and periodontitis. Thus, further investigations to elucidate the effect of TCA antidepressants on periodontitis in patients with both MetS and periodontitis are warranted.

In conclusion, the present study demonstrated for the first time that imipramine as an inhibitor of aSMase effectively abolished the synergy between MetS and LPS on alveolar bone loss and periodontal inflammation in animal model. This study also demonstrated that imipramine downregulates pro-inflammatory and pro-osteoclastogenic gene expression in macrophages *in vitro*, which is likely the mechanism underlying the inhibitory effect of imipramine on MetS-exacerbated periodontitis in animal model.

ACKNOWLEDGEMENTS

This work was supported by National Institutes of Health grant DE027070 and Department of Veterans Affairs, Veterans Health Administration, Office of Research and Development, Biomedical Laboratory Research and Development grant 5I01BX000854 (to Y.H.). This study utilized the facilities and resources of the MUSC Center for Oral Health Research.

DATA AVAILABILITY STATEMENT

The data that support the findings of this study are available from the corresponding author upon reasonable request.

REFERENCES

(1). Beck J, Garcia R, Heiss G, Vokonas PS, Offenbacher S. Periodontal disease and cardiovascular disease. J Periodontol 1996; 67: 1123–1137.

(2). Offenbacher S Periodontal diseases: pathogenesis. Ann Periodontol 1996; 1: 821–878. [PubMed: 9118282]

(3). Grundy SM, Brewer HB Jr., Cleeman JI, Smith SC Jr., Lenfant C. Definition of metabolic syndrome: Report of the National Heart, Lung, and Blood Institute/American Heart Association conference on scientific issues related to definition. Circulation 2004; 109: 433–438. [PubMed: 14744958]

(4). Grundy SM. Pre-diabetes, metabolic syndrome, and cardiovascular risk. J Am Coll Cardiol 2012; 59: 635–643. [PubMed: 22322078]

(5). Lalla E, Lamster IB, Drury S, Fu C, Schmidt AM. Hyperglycemia, glycoxidation and receptor for advanced glycation endproducts: potential mechanisms underlying diabetic complications, including diabetes-associated periodontitis. Periodontology 2000 2000; 23: 50–62. [PubMed: 11276765]

(6). Nibali L, Tatarakis N, Needleman I, et al. Clinical review: Association between metabolic syndrome and periodontitis: a systematic review and meta-analysis. J Clin Endocrinol Metab 2013; 98: 913–920. [PubMed: 23386648]

(7). Lamster IB, Pagan M. Periodontal disease and the metabolic syndrome. Int Dent J 2017; 67: 67–77. [PubMed: 27861820]

(8). Sima C, Viniegra A, Glogauer M. Macrophage immunomodulation in chronic osteolytic diseases-the case of periodontitis. J Leukoc Biol 2019; 105: 473–487. [PubMed: 30452781]

(9). Hienz SA, Paliwal S, Ivanovski S. Mechanisms of Bone Resorption in Periodontitis. J Immunol Res 2015; 2015: 615486. [PubMed: 26065002]

(10). Sima C, Glogauer M. Macrophage subsets and osteoimmunology: tuning of the immunological recognition and effector systems that maintain alveolar bone. Periodontol 2000 2013; 63: 80–101. [PubMed: 23931056]

(11). Jin J, Zhang X, Lu Z, et al. Acid sphingomyelinase plays a key role in palmitic acid-amplified inflammatory signaling triggered by lipopolysaccharide at low concentrations in macrophages. Am J Physiol Endocrinol Metab 2013; 305: E853–867. [PubMed: 23921144]

(12). Cascio G, Schiera G, Di Liegro I. Dietary fatty acids in metabolic syndrome, diabetes and cardiovascular diseases. Curr Diabetes Rev 2012; 8: 2–17. [PubMed: 22414056]

(13). Bauer J, Liebisch G, Hofmann C, et al. Lipid alterations in experimental murine colitis: role of ceramide and imipramine for matrix metalloproteinase-1 expression. PLoS One 2009; 4: e7197. [PubMed: 19787068]

(14). Schloer S, Brunotte L, Goretzko J, et al. Targeting the endolysosomal host-SARS-CoV-2 interface by clinically licensed functional inhibitors of acid sphingomyelinase (FIASMA) including the antidepressant fluoxetine. Emerg Microbes Infect 2020; 9: 2245–2255. [PubMed: 32975484]

(15). Kornhuber J, Tripal P, Reichel M, et al. Functional Inhibitors of Acid Sphingomyelinase (FIASMAs): a novel pharmacological group of drugs with broad clinical applications. Cell Physiol Biochem 2010; 26: 9–20. [PubMed: 20502000]

(16). Li Y, Lu Z, Zhang X, et al. Metabolic syndrome exacerbates inflammation and bone loss in periodontitis. J Dent Res 2015; 94: 362–370. [PubMed: 25503900]

(17). Yu H, Li Q, Herbert B, et al. Anti-inflammatory effect of MAPK phosphatase-1 local gene transfer in inflammatory bone loss. Gene therapy 2011; 18: 344–353. [PubMed: 21068780]

(18). Rogers JE, Li F, Coatney DD, et al. Actinobacillus actinomycetemcomitans lipopolysaccharide-mediated experimental bone loss model for aggressive periodontitis. J Periodontol 2007; 78: 550–558. [PubMed: 17335380]

(19). Jin J, Zhang X, Lu Z, et al. Simvastatin inhibits lipopolysaccharide-induced osteoclastogenesis and reduces alveolar bone loss in experimental periodontal disease. J Periodontal Res 2014; 49: 518–526. [PubMed: 24117880]

(20). Steinkamp HM, Hathaway-Schrader JD, Chavez MB, et al. Tristetraprolin Is Required for Alveolar Bone Homeostasis. J Dent Res 2018; 97: 946–953. [PubMed: 29514008]

(21). Bouxsein ML, Boyd SK, Christiansen BA, Guldberg RE, Jepsen KJ, Muller R. Guidelines for assessment of bone microstructure in rodents using micro-computed tomography. J Bone Miner Res 2010; 25: 1468–1486. [PubMed: 20533309]

(22). Park CH, Abramson ZR, Taba M Jr., et al. Three-dimensional micro-computed tomographic imaging of alveolar bone in experimental bone loss or repair. J Periodontol 2007; 78: 273–281. [PubMed: 17274716]

(23). Jin J, Machado ER, Yu H, et al. Simvastatin inhibits LPS-induced alveolar bone loss during metabolic syndrome. J Dent Res 2014; 93: 294–299. [PubMed: 24352501]

(24). Van Veldhoven PP, Bell RM. Effect of harvesting methods, growth conditions and growth phase on diacylglycerol levels in cultured human adherent cells. Biochim Biophys Acta 1988; 959: 185–196. [PubMed: 3349097]

(25). Polak D, Shapira L. An update on the evidence for pathogenic mechanisms that may link periodontitis and diabetes. J Clin Periodontol 2018; 45: 150–166. [PubMed: 29280184]

(26). Karmi A, Iozzo P, Viljanen A, et al. Increased brain fatty acid uptake in metabolic syndrome. Diabetes 2010; 59: 2171–2177. [PubMed: 20566663]

(27). Matsuo K, Ray N. Osteoclasts, mononuclear phagocytes, and c-Fos: new insight into osteoimmunology. Keio J Med 2004; 53: 78–84. [PubMed: 15247511]

(28). Shiozawa S, Tsumiyama K. Pathogenesis of rheumatoid arthritis and c-Fos/AP-1. Cell Cycle 2009; 8: 1539–1543. [PubMed: 19395871]

(29). Albouz S, Hauw JJ, Berwald-Netter Y, Boutry JM, Bourdon R, Baumann N. Tricyclic antidepressants induce sphingomyelinase deficiency in fibroblast and neuroblastoma cell cultures. Biomedicine 1981; 35: 218–220. [PubMed: 6285997]

(30). Lu Z, Li Y, Syn WK, et al. Amitriptyline inhibits nonalcoholic steatohepatitis and atherosclerosis induced by high-fat diet and LPS through modulation of sphingolipid metabolism. Am J Physiol Endocrinol Metab 2020; 318: E131–E144. [PubMed: 31821039]

(31). Marchesini G, Marzocchi R. Metabolic syndrome and NASH. Clin Liver Dis 2007; 11: 105–117, ix. [PubMed: 17544974]

(32). Bullon P, Morillo JM, Ramirez-Tortosa MC, Quiles JL, Newman HN, Battino M. Metabolic syndrome and periodontitis: is oxidative stress a common link? J Dent Res 2009; 88: 503–518. [PubMed: 19587154]

(33). Kitajima I, Soejima Y, Takasaki I, Beppu H, Tokioka T, Maruyama I. Ceramide-induced nuclear translocation of NF-kappa B is a potential mediator of the apoptotic response to TNF-alpha in murine clonal osteoblasts. Bone 1996; 19: 263–270. [PubMed: 8873967]

(34). Kim MH, Ahn HK, Lee EJ, et al. Hepatic inflammatory cytokine production can be regulated by modulating sphingomyelinase and ceramide synthase 6. Int J Mol Med 2017; 39: 453–462. [PubMed: 28035360]

(35). Li Y, Lu Z, Zhang L, Kirkwood KL, Lopes-Virella MF, Huang Y. Acid sphingomyelinase deficiency exacerbates LPS-induced experimental periodontitis. Oral Dis 2020; 26: 637–646. [PubMed: 31883406]

(36). Kim BJ, Lee JY, Park SJ, et al. Elevated ceramides 18:0 and 24:1 with aging are associated with hip fracture risk through increased bone resorption. Aging (Albany NY) 2019; 11: 9388–9404. [PubMed: 31675352]

(37). Bey A, Ahmad SS, Azmi SA, Ahmed S. Effect of antidepressants on various periodontal parameters: A case-control study. J Indian Soc Periodontol 2020; 24: 122–126. [PubMed: 32189839]

(38). Hasan F, Ikram R, Simjee SU, Iftakhar K, Asadullah K. Effects of 1% amitriptyline gel and mouthwash in patients with periodontal diseases via local drug delivery system: A randomized control clinical trial. Pak J Pharm Sci 2019; 32: 1855–1860. [PubMed: 31680083]

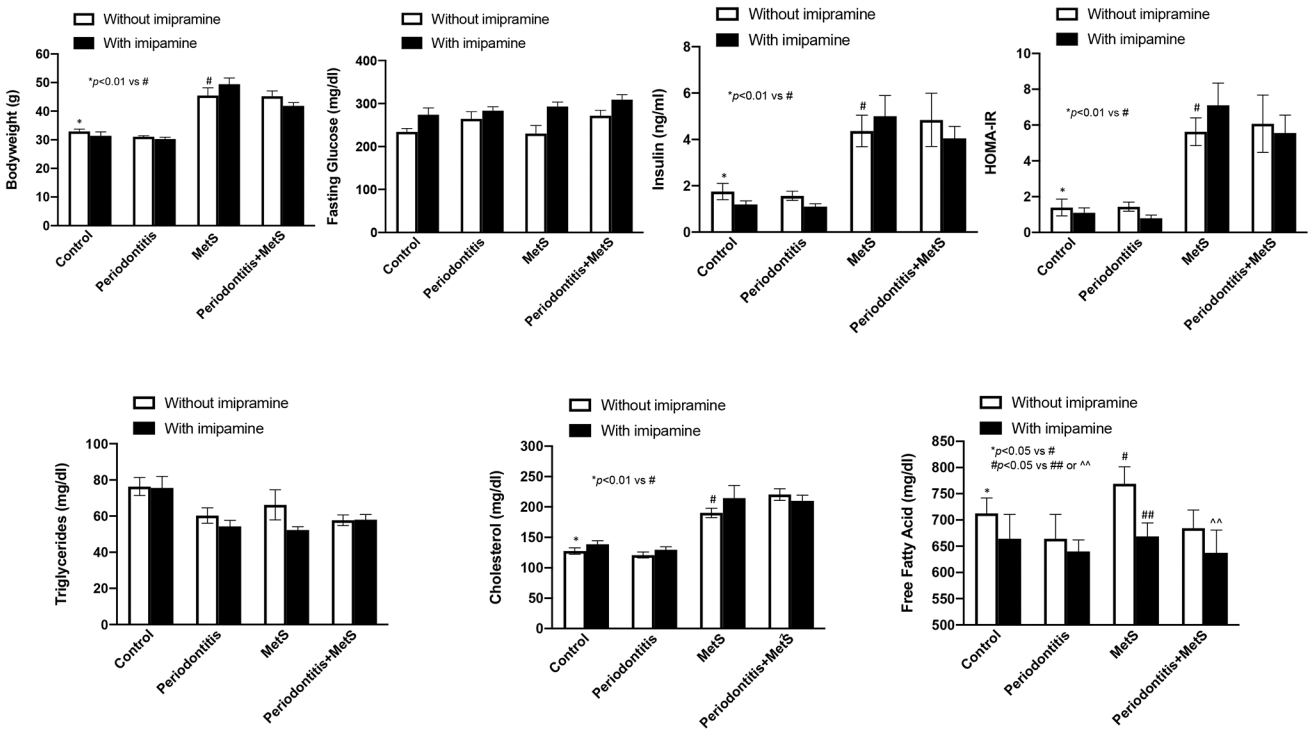

Figure 1.

The effect of imipramine on the metabolic parameters including bodyweight, glucose, insulin and insulin resistance (HOMA-IR), triglyceride, total cholesterol and free fatty acid in mice with or without periodontitis or metabolic syndrome (MetS). Six weeks old male C57BL/6 mice were fed HFD for 20 weeks to induce MetS and treated with LPS by periodontal injection in the last 4 weeks to induce periodontitis. Control mice were fed LFD or injected with PBS. Part of the mice were treated with imipramine 3 weeks before and 4 weeks during the LPS injection. At the end of the feeding and treatment, blood was collected, and the serum levels of the metabolic parameters were quantified. The data are mean ± SD (n=7–10).

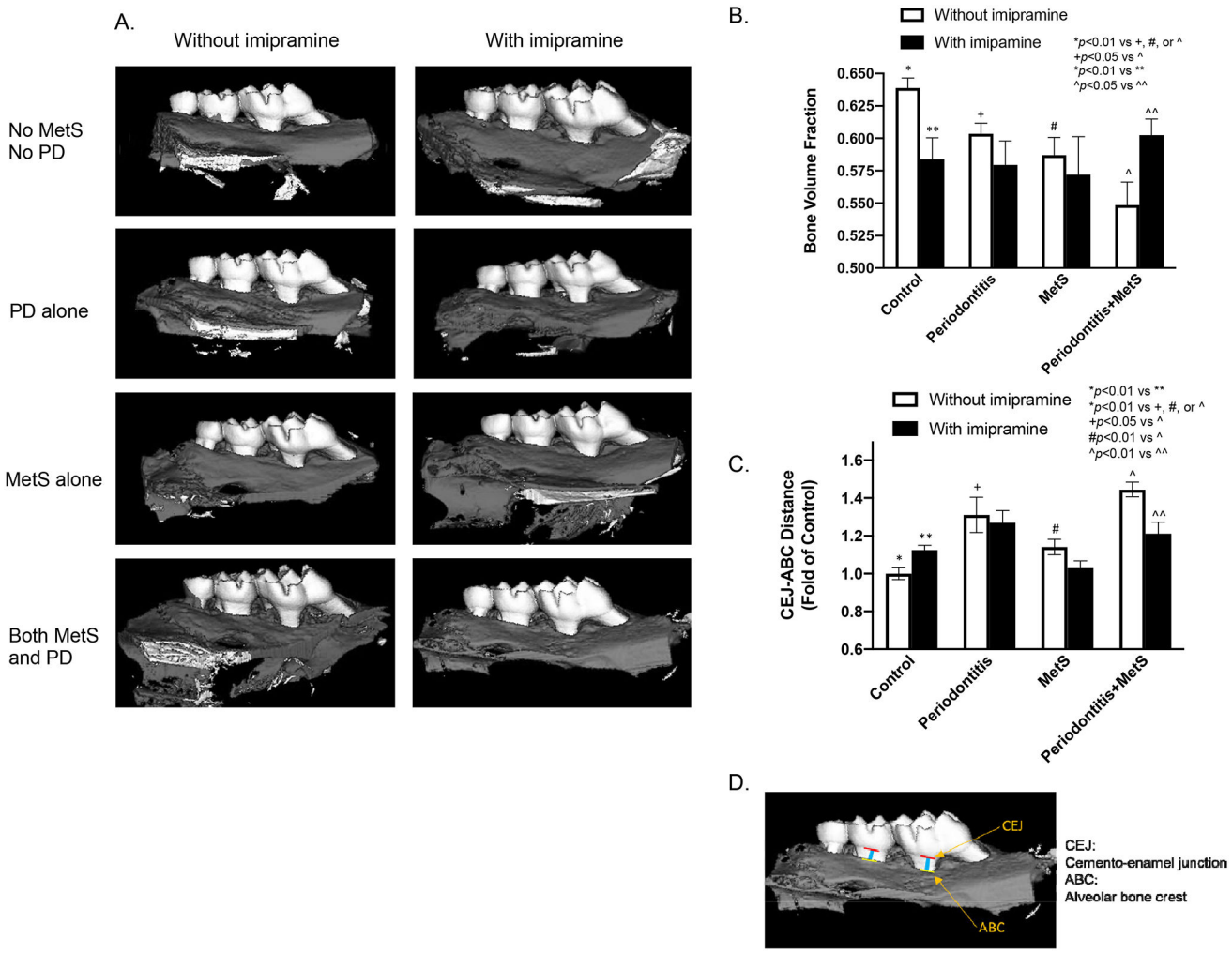

Figure 2.

The effect of imipramine on alveolar bone loss induced by LPS and/or metabolic syndrome (MetS). C57BL/6 mice were fed HFD for 20 weeks to induce MetS and/or treated with LPS for the last 4 weeks to induce periodontitis (PD). Control mice were fed LFD or injected with PBS. Half of mice were also treated with imipramine in the last 7 weeks as described in Methods. After the feeding and treatments, the maxillae were scanned with μCT. Representative μCT image (A) and bone volume fractions (B) for 8 groups are shown (B). In addition, the liner distances between CEJ to ABC for the first and second molars are shown (C). The CEJ and ABC as well as the distance between CEJ and ABC of the first and second molars were presented (Fig. 2D). The data are mean ± SD (n=7–10). CEJ, cement–enamel junction; ABC, alveolar bone crest.

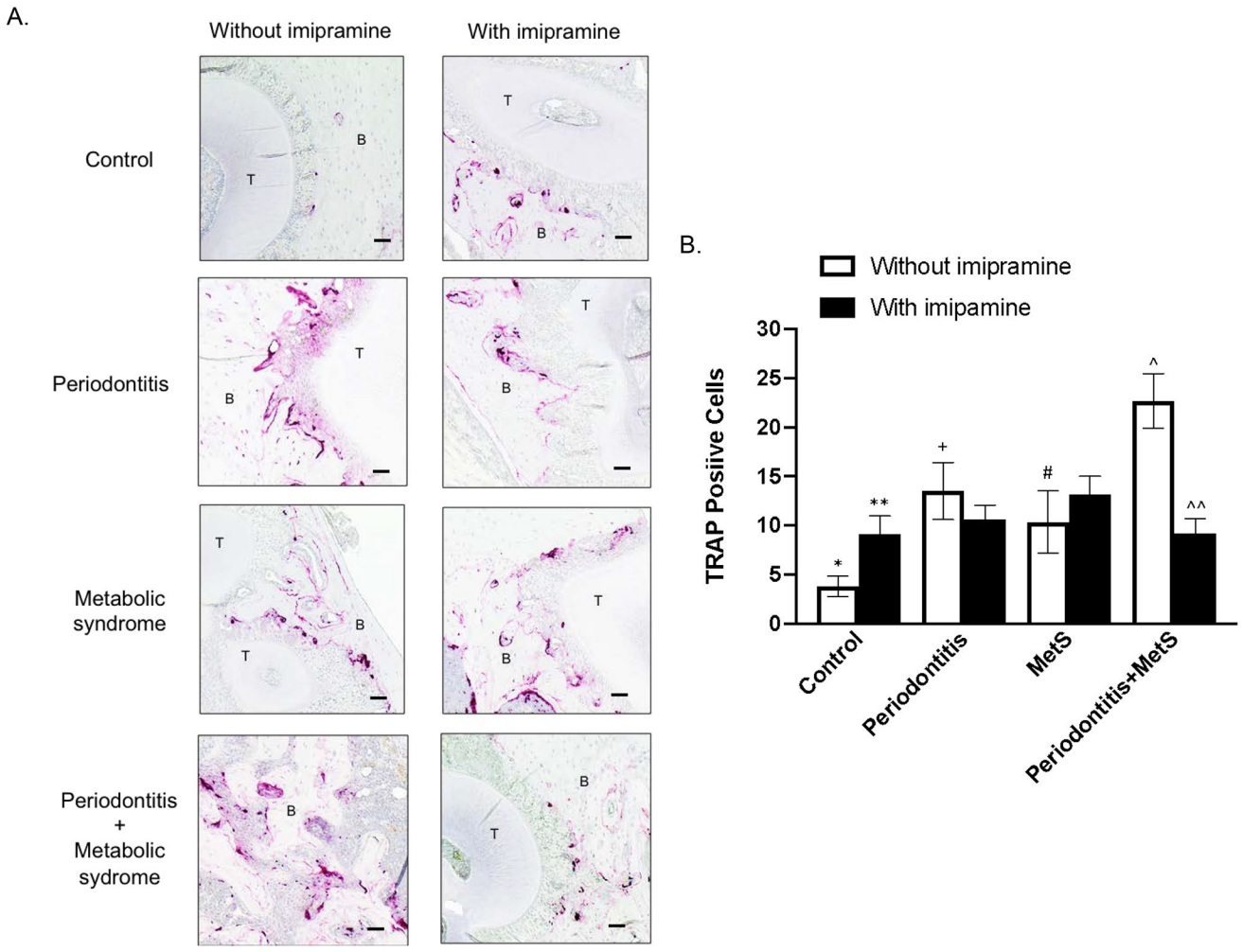

Figure 3.

The effect of imipramine on osteoclast formation and bone resorption induced by LPS and/or MetS. C57BL/6 mice were fed HFD for 20 weeks to induce MetS and/or treated with LPS for the last 4 weeks to induce periodontitis. Control mice were fed LFD or injected with PBS. Half of mice were also treated with imipramine in the last 7 weeks as described in Methods. The maxillae were decalcified and sectioned after being scanned by micro-computed tomography. Tartrate resistant and phosphatase (TRAP) staining to detect osteoclasts was performed on the tissue sections. Representative tissue sections with TRAP staining from 8 groups (A) and multinucleated TRAP-positive osteoclasts are shown (B). Photomicrographs were taken at 100x magnification. The data are mean ± SD (n=7–10). *p<0.05 vs **, *p<0.05 vs +, *p<0.05 vs #, *p<0.05 vs^, +p<0.05 vs ^, ^p<0.05 vs ^^. T: tooth; B: alveolar bone. Scale bar = 100 μm.

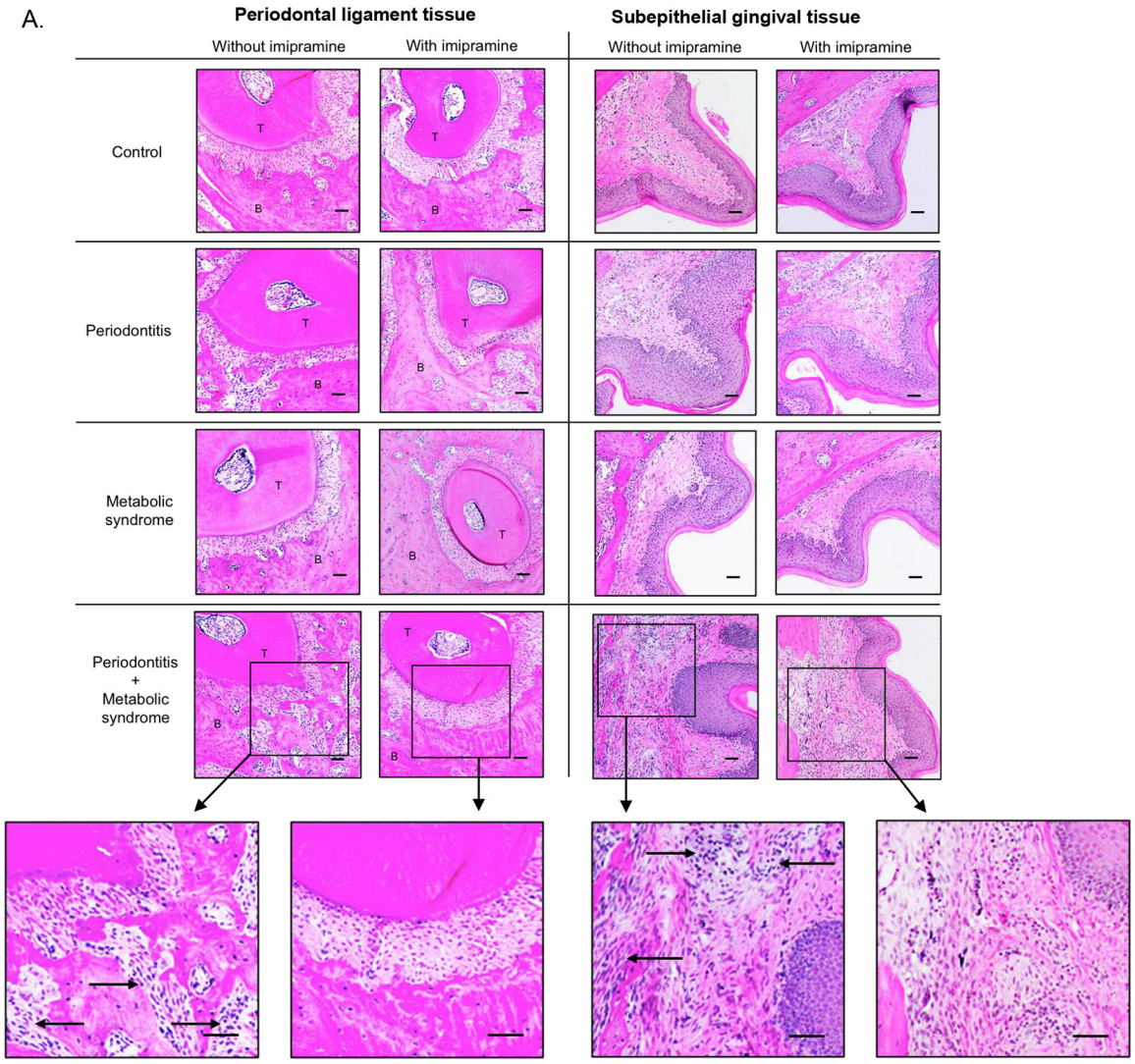

B.

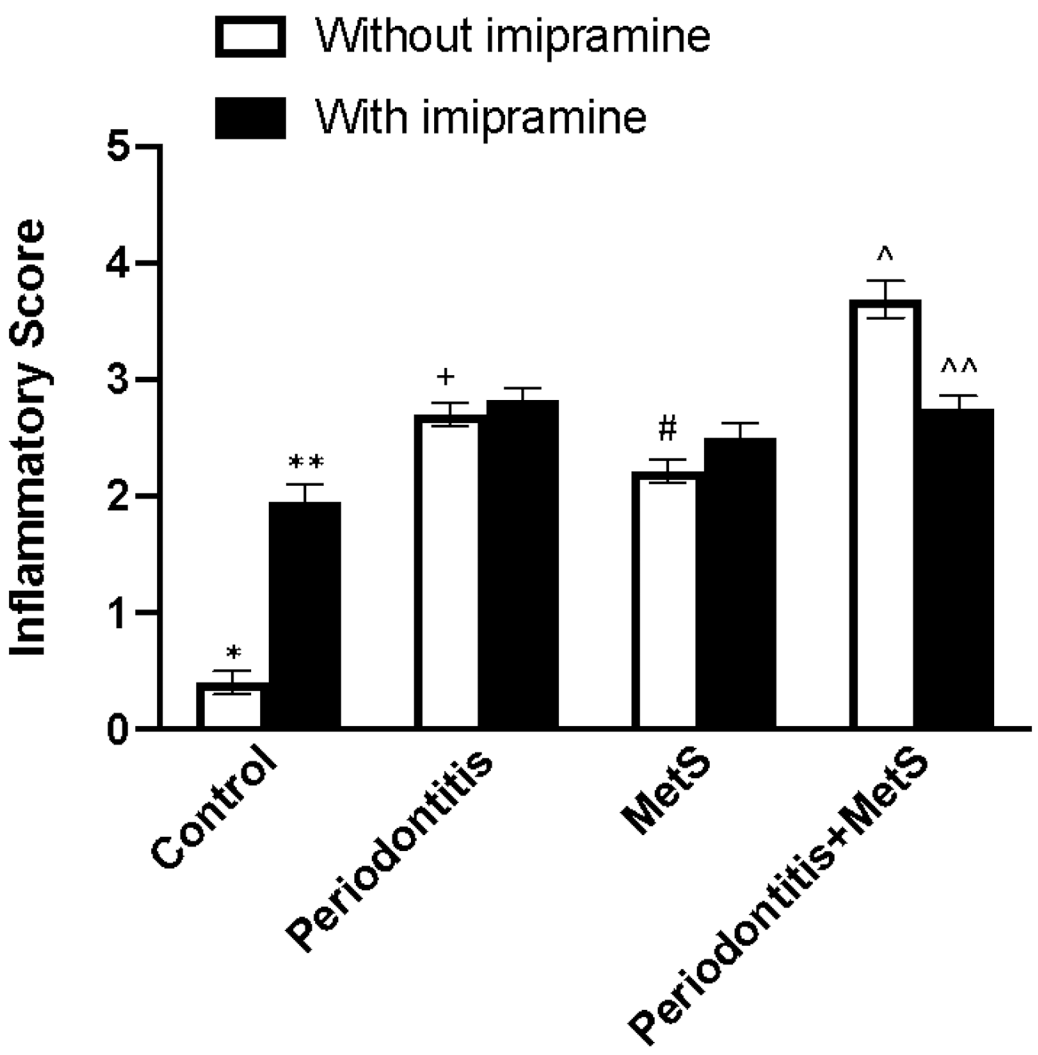

Figure 4.

The effect of imipramine on leukocyte infiltration induced by LPS and/or metabolic syndrome (MetS). In addition to TRAP staining as described above, the tissue sections were also stained with hematoxylin and eosin (H/E), and histological evaluation of leukocyte infiltration was performed. Representative tissue sections with H/E staining in periodontal ligament tissue or subepithelial gingival tissue are shown (A). Scale bar = 100 μm. Inset: Images were enlarged (scale bar=300 μm). The arrows indicate infiltrated leukocytes. The inflammatory scores were determined according to the degree of leukocyte infiltration and bone resorption as described in Materials and Methods (B). The data are mean ± SD (n=7–10). *p<0.01 vs **, *p<0.01 vs +, *p<0.01 vs #, *p<0.01 vs^, +p<0.01 vs ^, #p<0.01 vs ^. ^p<0.01 vs ^^. T: tooth; B: alveolar bone.

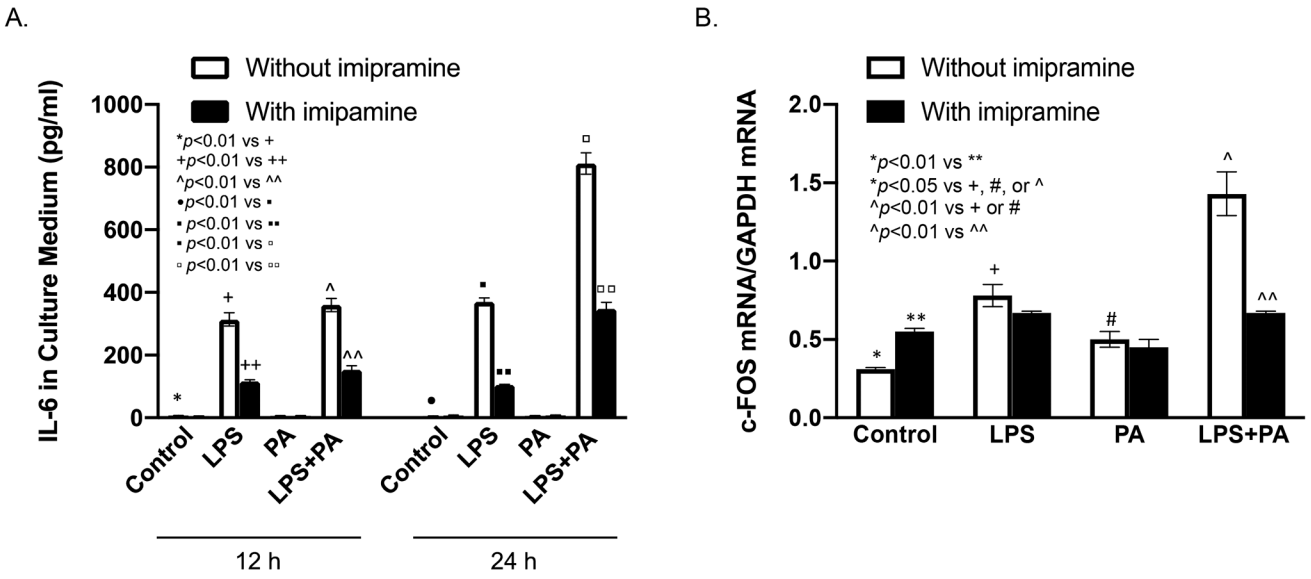

Figure 5.

The effect of imipramine on IL-6 secretion and c-FOS expression by macrophages stimulated with LPS and/or PA. RAW264.7 macrophages were treated with 1 ng/ml of LPS, 100 μM of PA or both LPS and PA. The levels of IL-6 in culture medium after 12 and 24 h incubation (A), and c-FOS mRNA at 12 h (B) were quantified using ELISA and real-time PCR, respectively. The data are mean ± SD of one of three experiments with similar results.

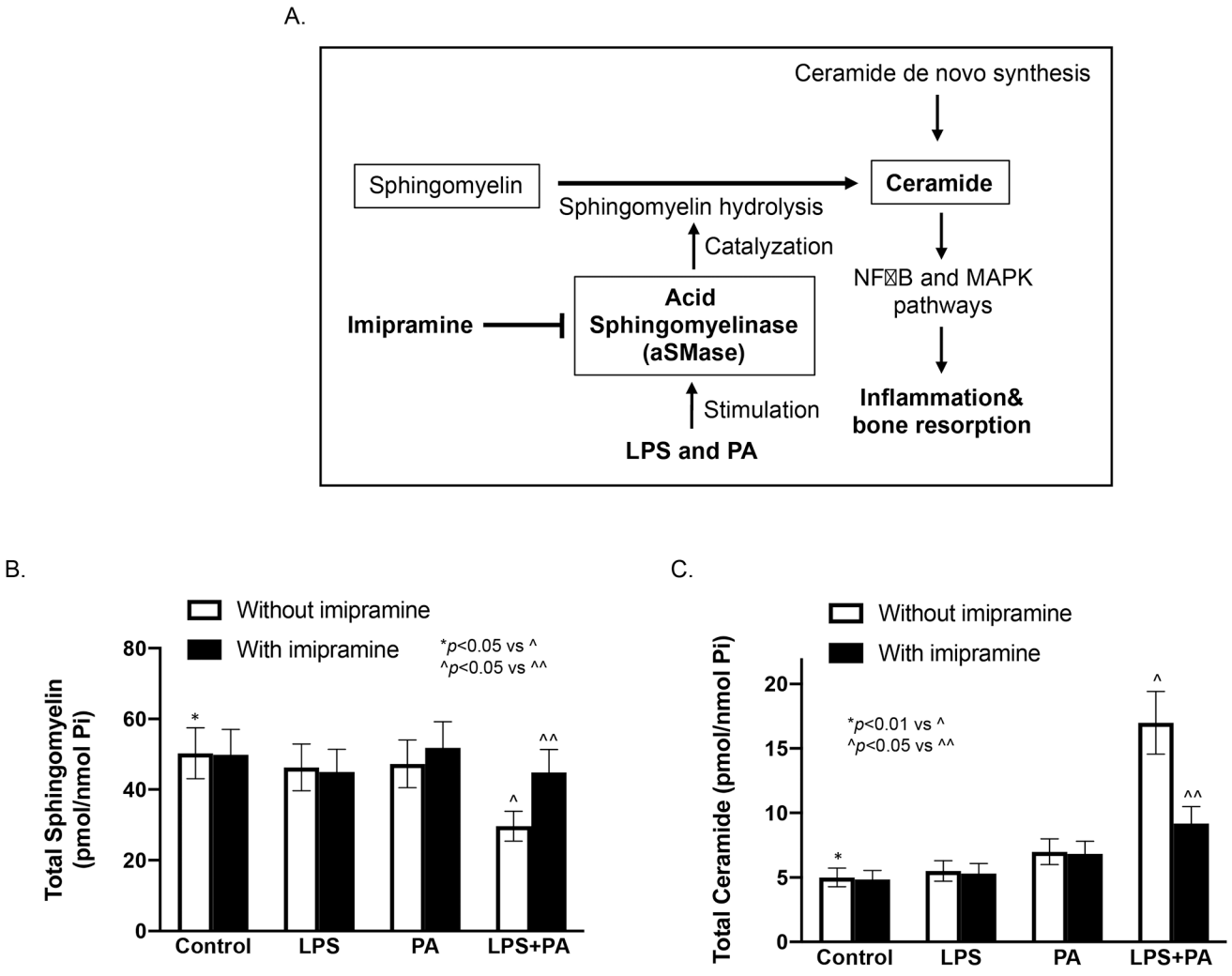

Figure 6.

The effect of imipramine on ceramide (CER) and sphingomyelin (SM) contents in macrophages stimulated with LPS and/or PA. A. Schematic diagram shows how imipramine inhibits aSMase-catalyzed SM hydrolysis and thus decreases CER production. The reduction of CER production decreases periodontal inflammation and bone resorption. B and C. The effect of imipramine on celluar contests of SM (A) and CER (B) in RAW264.7 macrophages stimulated with LPS and/or PA. The cells were treated with 1 ng/ml of LPS, 100 μM of PA or both LPS and PA for 24 h. After the treatments, cellular SM and CER contents were quantified with lipidomics as described in Methods. The data are mean ± SD (n=2). Pi, phosphate.

Table 1.

The effect of imipramine on expression of genes involved in periodontal inflammation and osteoclastogenesis in macrophages treated with LPS, PA or LPS plus PA

	Fold changes for cells treated in the absence of imipramine				Fold changes for cells treated in the presence of imipramine			
	Control	**LPS**	**PA**	**LPS + PA**	**Imipramine**	**LPS + imipramine**	**PA + imipramine**	**LPS + PA + imipramine**
Fos	1.00	1.84	1.11	4.31	1.18	2.15	1.24	0.18
Il1a	1.00	9.65	0.39	32.99	0.75	10.05	0.71	19.64
Il1b	1.00	51.55	0.61	170.84	0.55	19.80	0.81	10.15
Myd88	1.00	1.13	0.88	1.20	0.97	1.38	0.73	0.76
Ptgs2	1.00	12.16	0.88	19.69	1.65	11.83	2.71	12.90
Tnf	1.00	3.48	0.74	5.61	1.72	5.07	1.32	3.73

Abbreviations: PA, palmitic acid; CSF2, colony-stimulating factor 2; Cxcl10, C-X-C motif chemokine 10; II1a, interleukin 1 alpha; II1b, interleukin 1 beta; Myd88, myeloid differentiation factor 88; Ptgs2, prostaglandin-Endoperoxide Synthase 2; Tnf, tumor necrosis factor.

RAW 264.7 cells were treated with 1 ng/ml LPS, 100 μM PA, or both in the presence or absence of 50 μM of IMP for 24 h. After treatment, cells were harvested and subjected to PCR array study, as described in MATERIALS AND METHODS. The GAPDH mRNA was used as a housekeeping gene. To compare the gene expression in cells treated with LPS, PA, or LPS plus PA with that in control cells, ΔC_T was first calculated by the following formula: $\Delta C_T = C_T$ in treated cells - C_T in control cells. The gene expression in cells treated with LPS, PA, or both in the absence or presence of imipramine was presented as the fold of the control gene expression and calculated as $2^{\Delta CT}$.

Table 2.

The effect of imipramine (IMP) on sphingomyelin (SM) content in macrophages treated with LPS, PA or LPS plus PA

Treatment	IMP	C16-SM	C18-SM	C20-SM	C22-SM	C24-SM	C24:1-SM	Total SM
Control	− IMP	31.79±4.54	1.85±0.27	0.62±0.09	3.27±0.47	2.36±0.34	6.56±0.94	50.32±7.19¶
	+ IMP	31.85±7.19	2.15±0.31	0.72±0.10	3.57±0.51	2.24±0.32	5.80±0.83	49.90±7.13
LPS	− IMP	31.18±4.46	1.45±0.21	0.51±0.07	2.56±0.37	1.88±0.27	4.82±0.69	46.29±6.61#
	+ IMP	30.09±4.30	1.77±0.25	0.57±0.08	2.84±0.41	2.23±0.32	4.31±0.62	45.01±6.43
PA	− IMP	24.78±3.54	3.95±3.54	1.24±0.18	5.58±0.80	2.37±0.34	6.42±0.92	47.30±6.76^
	+ IMP	31.07±4.44	3.63±0.52	1.01±0.15	4.66±0.67	2.1±0.30	6.31±0.90	51.84±7.41
LPS+PA	− IMP	17.59±2.51	2.06±0.30	0.60±0.09	2.57±0.37	1.07±0.15	3.89±0.56	29.68±4.24*
	+ IMP	28.59±4.09	2.58±0.37	0.76±0.11	3.29±0.47	1.470.21	5.45±0.78	44.93±6.42+

Raw264.7 cells were treated with 1 ng/ml of LPS, 100 μM of PA or both LPS and PA in the presence or absence of 50 μM of IMP for 12 h. After treatment, cells were harvested and subjected to the lipidomic analysis of SMs as described in Methods. The unit of the values is pmol/nmol Pi. IMP, imipramine; SM, sphingomyelin; PA, palmitic acid.

* $p<0.01$ vs +, ¶, # or ^.

Table 3.

The effect of imipramine (IMP) on ceramide (CER) content in macrophages treated with LPS, PA or LPS plus PA

Treatment	IMP	C16-CER	C18-CER	C20-CER	C22-CER	C24-CER	C24:1-CER	Total CER
Control	− IMP	0.74±0.11	0.05±0.01	0.03±0.01	0.36±0.05	2.24±0.32	1.44±0.21	5.00±0.72¶,
	+ IMP	0.96±0.14	0.13±0.02	0.04±0.01	0.46±0.07	1.69±0.24	1.41±0.20	4.85±0.69
LPS	− IMP	1.16±0.17	0.06±0.01	0.03±0.01	0.34±0.05	2.21±0.32	1.52±0.22	5.51±0.79#
	+ IMP	1.33±0.19	0.11±0.02	0.05±0.01	0.43±0.06	2.00±0.29	1.22±0.18	5.31±0.76
PA	− IMP	1.52±0.22	0.28±0.04	0.17±0.03	1.54±0.22	1.98±0.28	1.32±0.19	7.00±1.00
	+ IMP	2.08±0.30	0.46±0.07	0.23±0.03	1.61±0.23	1.57±0.23	0.76±0.11	6.83±0.98^
LPS+PA	− IMP	4.84±0.69	1.23±0.18	0.66±0.10	3.56±0.51	3.37±0.48	2.72±0.39	17.00±2.43*
	+ IMP	3.08±0.44	0.62±0.09	0.28±0.04	1.94±0.28	1.88±0.27	1.16±0.17	9.19±1.31+

Raw264.7 cells were treated with 1 ng/ml of LPS, 100 μM of PA or both LPS and PA in the presence or absence of 50 μM of IMP for 12 h. After treatment, cells were harvested and subjected to the lipidomic analysis of CERs as described in Methods. The unit of the values is pmol/nmol Pi. IMP, imipramine; CER, ceramide; PA, palmitic acid.

* $p<0.01$ vs +, ¶, # or ^.